Biosensors and Bioelectronics 38 (2012) 289–294

Contents lists available at SciVerse ScienceDirect

Biosensors and Bioelectronics

journal homepage: www.elsevier.com/locate/bios

A high-sensitive and fast-fabricated glucose biosensor based on Prussian blue/topological insulator Bi_2Se_3 hybrid film

Shouguo Wu [a,*], Gang Liu [a], Ping Li [a], Hao Liu [a], Haihong Xu [b]

[a] Department of Chemistry, University of Science and Technology of China, Hefei 230029, PR China
[b] Clinical Laboratory, Hefei Third People's Hospital, Hefei 230022, PR China

ARTICLE INFO

Article history:
Received 10 April 2012
Received in revised form
30 May 2012
Accepted 3 June 2012
Available online 16 June 2012

Keywords:
Glucose biosensor
Topological insulator
Bi_2Se_3
Prussian blue
Hybrid film

ABSTRACT

A novel and fast-fabricated Prussian blue (PB)/topological insulator Bi_2Se_3 hybrid film has been prepared by coelectrodeposition technique. Taking advantages of topological insulator in possessing exotic metallic surface states with bulk insulating gap, Prussian blue nanoparticles in the hybrid film have smaller size as well as more compact structure, showing excellent pH stability even in the alkalescent solution of pH 8.0. Based on the Laviron theory, the electron transfer rate constant of PB/Bi_2Se_3 hybrid film modified electrode was calculated to be $4.05 \pm 0.49\ s^{-1}$, a relatively big value which may be in favor of establishing a high-sensitive biosensor. An amperometric glucose biosensor was then fabricated by immobilizing glucose oxidase (GOD) on the hybrid film. Under the optimal conditions, a wide linear range extending over 3 orders of magnitude of glucose concentrations (1.0×10^{-5}–1.1×10^{-2} M) was obtained with a high sensitivity of 24.55 μA mM^{-1} cm^{-2}. The detection limit was estimated for 3.8 μM defined from a signal/noise of 3. Furthermore, the resulting biosensor was applied to detect the blood sugar in human serum samples without any pretreatment, and the results were comparatively in agreement with the clinical assay.

1. Introduction

The birth of topological insulators opened up an important new family of materials which possess exotic metallic surface states with bulk insulating gap, providing an avenue for dissipationless quantum electronics and room temperature spintronics applications such as fault-tolerant quantum computing (Moore, 2009, 2010). In topological insulators, strong spin–orbit coupling induces nontrivial surface states that are robustly protected against any time reversal perturbations, such as crystal defects and nonmagnetic impurities (Bernevig et al., 2006; Fu and Kane, 2007; König et al., 2007; Moore, 2010). Recent theoretical calculations and photoemission spectroscopy measurements on bulk A_2B_3 (A=Bi; B=Se, Te) materials which were previously studied for more than half a century as infrared detections and thermoelectric applications show that they are just about the three-dimensional topological insulators and thus the research interest in these materials dramatically increases (Harman et al., 1957; Satterthwaite and Ure, 1957; Zhang et al., 2009).

As a narrow gap semiconductor, the surface states of Bi_2Se_3 forms a single Dirac cone inside a large bulk band gap of 0.3 eV, being suggested as the reference material for three-dimensional topological insulators (Moore, 2009; Xia et al., 2009; Zhang et al., 2009). Many methods have been employed to synthesize this eyes-attractive material, especially the nanoscale one which has a large surface-to-volume ratio that can manifest the conductive surface states. For examples, Bi_2Se_3 nanobelts have been synthesized by sonochemical methods (Cui et al., 2004), Bi_2Se_3 nanoplates by solvothermal synthesis (Wang et al., 2003) and metal-organic chemical vapor deposition (Lin et al., 2007). Vapor–liquid–solid (VLS) growth has also been proved to be an effective approach to produce high quality Bi_2Se_3 nanowires and nanoribbons (Kong et al., 2009). Complicated procedure and expensive cost, however, were hardly avoidable when using these methods. Electrochemical synthesis is well known for its advantages in saving time, reducing cost and controlling scale. It is simple and inexpensive for the preparation of high quality thin film. Besides, many reports were focused on the thermoelectric properties of Bi_2Se_3. However, the electrochemical properties, especially the peculiar effect during the procedure of co-electrodeposition, have rarely been reported.

Diabetes mellitus is a worldwide public health problem which is one of the most leading causes of death and disability in the world. The diagnosis and control of diabetes mellitus requires an accurate and tight monitoring of blood glucose concentration (Reach and Wilson, 1992). There are millions of diabetics who need to test their blood glucose level daily, which makes a huge market size (Wang, 2007). Therefore, fascinating research and

* Corresponding author. Tel.: +86 551 3492126.
E-mail address: sgwu@ustc.edu.cn (S. Wu).

0956-5663/$ - see front matter © 2012 Elsevier B.V. All rights reserved.
http://dx.doi.org/10.1016/j.bios.2012.06.001

innovative detection strategies of glucose biosensors were intensively provided to realize reliable and urgent glycemic control (Wang, 2002, 2007). Among many types of biosensors, amperometric enzyme electrodes based on glucose oxidase (GOD) have always played a leading role (Karyakin et al., 1995). Known as the "artificial peroxidase", Prussian blue (PB) has been widely employed in fabricating the amperometric glucose biosensors due to its excellent catalytic properties toward reduction of hydrogen peroxide at low overpotential (Karyakin et al., 2000). Furthermore, PB nanoparticles have caught many eyeballs due to their interesting magnetic, electrical, optical, and chemical properties that cannot be achieved by their bulk counterparts (Domínguez-Vera and Colacio, 2003). As to PB based biosensors, nanostructured Prussian blue modified electrodes demonstrate a significantly decreased background as well as a low detection limit, which resulted in improving the properties of sensors (Karyakin et al., 2004). Thus it is a convenient way to fabricate superior biosensors by means of reducing the size of Prussian blue particles.

Herein, we report a novel glucose biosensor based on Prussian blue/topological insulator Bi_2Se_3 hybrid film, with high sensitivity and fast fabrication. Taking the advantages of topological insulator in possessing exotic metallic surface states with bulk insulating gap, Prussian blue nanoparticles were easily synthesized with smaller size as well as more compact structure by being co-electrodeposited with topological insulator Bi_2Se_3. Furthermore, human serum samples were assayed to demonstrate the practical applicability of this new type of glucose biosensor.

2. Experimental

2.1. Apparatus

All electrochemical experiments were performed on a LK2005 Electrochemistry Work Station (LANLIKE Co. Ltd., Tianjin, China). A conventional three-electrode configuration was employed, consisting of the modified glassy carbon electrode (GCE, 3 mm in diameter) as the working electrode, a saturated calomel electrode as the reference electrode and a platinum wire as the counter electrode. Phosphate buffer solution (0.025 M KH_2PO_4/K_2HPO_4, pH 6.86) containing 0.1 M KCl was used as the supporting electrolyte. All electrochemical measurements were carried out at room temperature.

Scanning electron microscopy (SEM) was performed on a JEOL JSM-6700F SEM system to characterize the morphologies of the resulting Prussian blue film, Bi_2Se_3 film and PB/Bi_2Se_3 hybrid film modified electrodes. XRD patterns were recorded via a Philips X'Pert PRO S X-ray diffractometer with Cu K_α radiation ($\lambda = 1.5406$ Å).

2.2. Reagents

All chemicals used were of analytical grade and were used without any further purification. Bismuth nitrate pentahydrate ($Bi(NO_3)\cdot 5H_2O$), selenium dioxide (SeO_2), nitric acid (HNO_3), potassium ferricyanide ($K_3Fe(CN)_6$), potassium chloride (KCl), ferric chloride ($FeCl_3$), L-cysteine, L-cystine, L-histidine and hydrogen peroxide (H_2O_2,30% wt%) were all purchased from GUOYAO group Co. (Shanghai, China). The exact concentration of hydrogen peroxide was determined by titration with potassium permanganate. Uric acid and ascorbic acid were from Shanghai Chemical Reagents (Shanghai, China). Dopamine and glucose oxidase (GOD, EC 1.1.3.4, lyophilized powder, 245U mg^{-1}) from Shanghai YUANJU Co. (Shanghai, China) were produced by Sigma. Glucose stock solution (0.1 M) were prepared and allowed to mutarotate at room temperature for 24 h before use.

2.3. Fabrication of PB/Bi_2Se_3 hybrid film electrode

Prior to the surface modification, the glassy carbon electrode was polished first on wet fine emery SiC abrasive paper and then with alumina slurries (0.3 μm) until a mirror finish was observed. After that, it was rinsed thoroughly with deionized water and dried with N_2.

Solution A was the electrodepositing solution of Bi_2Se_3, which was a mixture of 2 mM $Bi(NO_3)\cdot 5H_2O$ and 3 mM SeO_2 in diluted nitric acid ($V(HNO_3):V(H_2O)=1:20$). Solution B was of Prussian blue, a mixture of 2 mM $K_3Fe(CN)_6$, 2 mM $FeCl_3$, 0.1 M KCl and 10 mM HCl. Solution C was a mixture of 0.1 M KCl and 10 mM HCl, used for activation. Co-electrodepositing solution was obtained by mixing 1 mL of solution A with 2 mL of solution B, followed by sonication for homodisperse. Hybrid film was electrodeposited onto the fresh surface of GCE by cyclic voltammetry, scanning from +0.60 V to −0.20 V at 50 mV s^{-1} for 20 cycles. After being washed, the modified electrode was transferred into solution C to activate by cycling from +0.35 V to −0.05 V at a rate of 50 mV s^{-1} for 30 times to obtain a stable voltammogram. The electrode surface was then rinsed with deionized water and dried in air.

2.4. Fabrication of the GOD-CS/PB/Bi_2Se_3 biosensor

0.5% chitosan solution was prepared by dissolving 0.5 g CS in 100 mL 2% acetic acid with stirring. The glucose biosensor was further fabricated by dropping 10 μL of 5 mg mL^{-1} GOD-CS onto the surface of modified electrode prepared in 2.3 and then dried in flowing air at room temperature. The whole period to prepare a batch of thus-fabricated biosensors could be limited in 1 h. The resulting biosensors were then stored in the phosphatic buffer at 4 °C before use.

3. Results and discussion

3.1. The cyclic voltammograms of co-electrodeposition procedure

As we know, the potentiostatic method has been widely used to prepare Bi_2Se_3 film (Subramanian and Padiyan, 2008; Torane and Bhosale, 2001; Xiao et al., 2008). To date, however, few reports mentioned to employ cyclic voltammetry to obtain stable Bi_2Se_3 films. Compared to the potentiostatic method, CV technique has its own advantages. In the oxidation and reduction process, dissolution and electrodeposition of films occurs alternately, so the deposited films are very compact and can adhere firmly to the electrode surface (Cui et al., 2002). On the other hand, CV technique takes unique advantages in coelectrodepositon of hybrid film. The typical cyclic voltammograms for the electrochemical co-deposition of Prussian blue and Bi_2Se_3 are illustrated in Fig. 1. As can be seen, two pairs of redox peaks can be distinguished at potentials around 0.21 V and 0.40 V respectively. The former is attributed to the redox of Prussian blue (Wu et al., 2010) and the later redox pair may correspond to the nitric acid in electrodepositing solution. Besides, an irreversible peak was also observed at about −0.11 V. In comparison with the CV obtained for control experiments under the same conditions in the absence of Bi_2Se_3 electrodepositing solution and in combination with previous study (Peng et al., 2011), the assignment of this reduction peak is attributed to the formation of Bi_2Se_3, which is described by Eq. (1) (see SFig. 1). Bi^{3+} promotes the H_2SeO_3 reduction because there is a large Gibbs free energy of the bismuth selenides (Peng et al., 2011).

$$3H_2SeO_3 + 2Bi^{3+} + 12H^+ + 18e^- = Bi_2Se_3 + 9H_2O \quad (1)$$

With number of scan cycles increased, the peak current of the redox couple of Prussian blue increased slowly, which means the

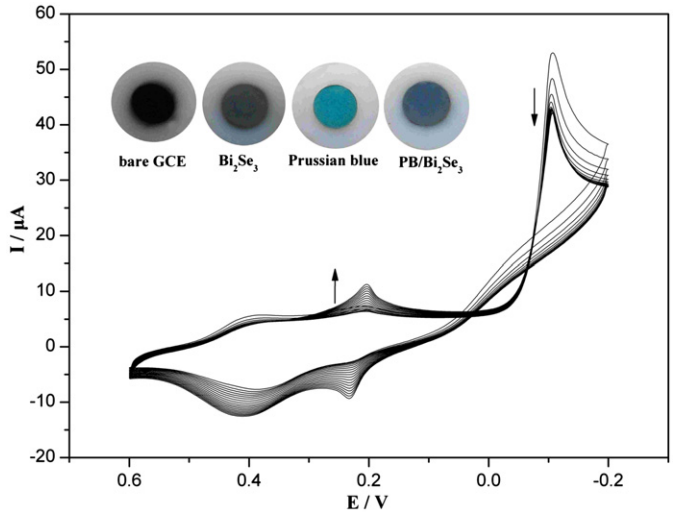

Fig. 1. Cyclic voltammograms of the coelectrodeposition of PB/Bi_2Se_3 hybrid film. CV conditions: 20 times recycling in the range from 0.60 to −0.20 V at a scan rate of 50 mV s^{-1}. Inset shows the digital photographs of different electrodes.

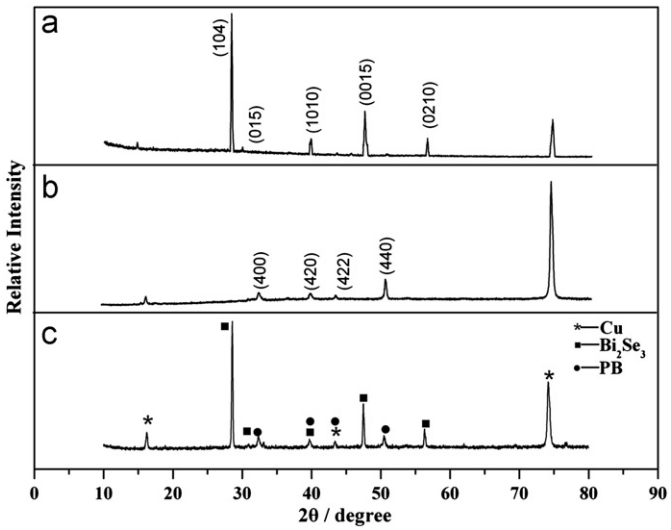

Fig. 2. XRD patterns of (a) Bi_2Se_3, (b) Prussian blue and (c) PB/Bi_2Se_3 films electrodeposited on copper sheets with the same electrodepositing condition.

continuous growth of well-conductive Prussian blue. Differently, the peak current for the deposition of bismuth selenide decreased quickly during the first 5 cycles and then reached a stable value. This is attributed to the bulk insulating property of the topological insulator Bi_2Se_3. As a reference material for the newly discovered three-dimensional topological insulators, the bulk Bi_2Se_3 material has been proved unambiguously to possess topologically protected conducting surface states with nondegenerate spins, which resided inside the bulk band gap (Cha et al., 2010). The increasing size of Bi_2Se_3 particles leads to the decreasing percentage of conducting surface states, resulting in a sudden decrease of conductivity. Inset of Fig. 1 is the digital photos of different modified electrodes, giving the electrode surface morphology. Judging from the color, PB/Bi_2Se_3 film shows the hybrid characteristic from both Bi_2Se_3 and Prussian blue films, indicating the successful deposition of the PB/ Bi_2Se_3 hybrid film on the bare GCE.

3.2. Characterization of the PB/ Bi_2Se_3 hybrid film

X-ray diffraction patterns of the as-deposited hybrid and contrast films (see Fig. 2) matched well with the standard pattern (JCPDS card no. 73-0687 for Prussian blue and no. 33-0214 for Bi_2Se_3). The XRD pattern of as-deposited Bi_2Se_3 thin film in Fig. 2(a) shows peaks at $2\theta=28.10^\circ$, 29.82°, 39.62°, 47.32° and 56.48° corresponding to reflections of (104), (015), (1010), (1015) and (0210) planes respectively with the preferred orientation along the (104) direction. Fig. 2(b) shows the XRD pattern of Prussian blue film with peaks at $2\theta=32.33^\circ$, 39.89°, 43.47° and 50.11°, which correspond to the (400), (420), (422), (440) reflections and could be indexed as pure face-centered-cubic phase of PB. When the co-electrodeposition was achieved, the XRD curve (Fig. 2(c)) contains their characteristic peaks of Bi_2Se_3 and PB, indicating the successful formation of hybrid film.

The surface morphologies of the modified electrodes were also investigated with scanning electron microscopy (SEM). Fig. 3(A) and (B) give the morphological images of Prussian blue and PB/Bi_2Se_3 films on GCE. Compared to the SEM image of pure PB, two prominent merits emerged which may be due to the effect of topological insulator Bi_2Se_3. First, according to the statistics of partical size from SEM images (see SFig. 2), the statistic average diameter of the particles became smaller from 22.93 nm of PB to 16.18 nm of PB/Bi_2Se_3, which is much smaller than 35 (± 8) nm of electrodeposited Prussian blue on graphite electrode (Haghighi et al., 2010). It seems that the difference of diameters is not so significant. However, the pure PB film showed serious aggregation under the same electrodepositing conditions as the hybrid film, which means the effective size of pure PB particles is much larger than 22.93 nm. In other words, the nano-size effect was improved when PB was coelectrodepositied with Bi_2Se_3. Second, what's more important is that a much smoother surface without obvious defect was observed from the image of PB/ Bi_2Se_3 film, which would be unquestionably beneficial to the stability of the hybrid film. According to the SEM of Bi_2Se_3 film electrodeposited on GCE (see SFig. 3), nano-scale topological insulator material Bi_2Se_3 had a large surface-to-volume ratio that can manifest the conductive metallic surface states (Kong et al., 2009).

Cyclic voltammetry was utilized to characterize the electrochemical behavior of PB which coexisted with Bi_2Se_3 on electrode surface. With increasing scan rate from 10 to 100 mV s^{-1}, the anodic and cathodic peak currents increased linearly (see SFig. 4), indicating the redox process of Prussian blue in this hybrid film was a reversible and surface-controlled process. Besides, the peak-to-peak separation was almost constant with different scan rates, indicating a fast electron transfer rate. According to the Laviron theory (Laviron, 1979) and table look-up method (m value), the electron transfer rate constant k_s was calculated to be 4.05 ± 0.49 s^{-1} (degree of confidence $t=95\%$), a relatively big value which may be in favor of establishing a high-sensitive biosensor.

3.3. Stability of PB/Bi_2Se_3 hybrid film in neutral and alkalescent solution

As is well known, the optimal acidity for most enzymes is within the pH range of 6.5–8.0 while PB is famous for its instability and dissolubility at pH values above 7.0, suggesting a limited application of PB modified electrode in acidic solution (Karyakin, 2001). But the PB/Bi_2Se_3 hybrid film is stable enough in neutral and alkalescent solution. Cyclic voltammetry was chosen to examine the stability by measuring the decrease in the redox peak currents during potential cycling in the buffer solutions with different pHs. Fig. 4 summarizes the response of voltammetric peak current of PB/Bi_2Se_3 modified electrode upon the pH of buffer solution. The results show that the PB/Bi_2Se_3 hybrid film can improve the stability of PB during the raise of pH and keep the activity in neutral and weak alkaline solution. Compact PB films of chemical deposition have been demonstrated to be highly stable

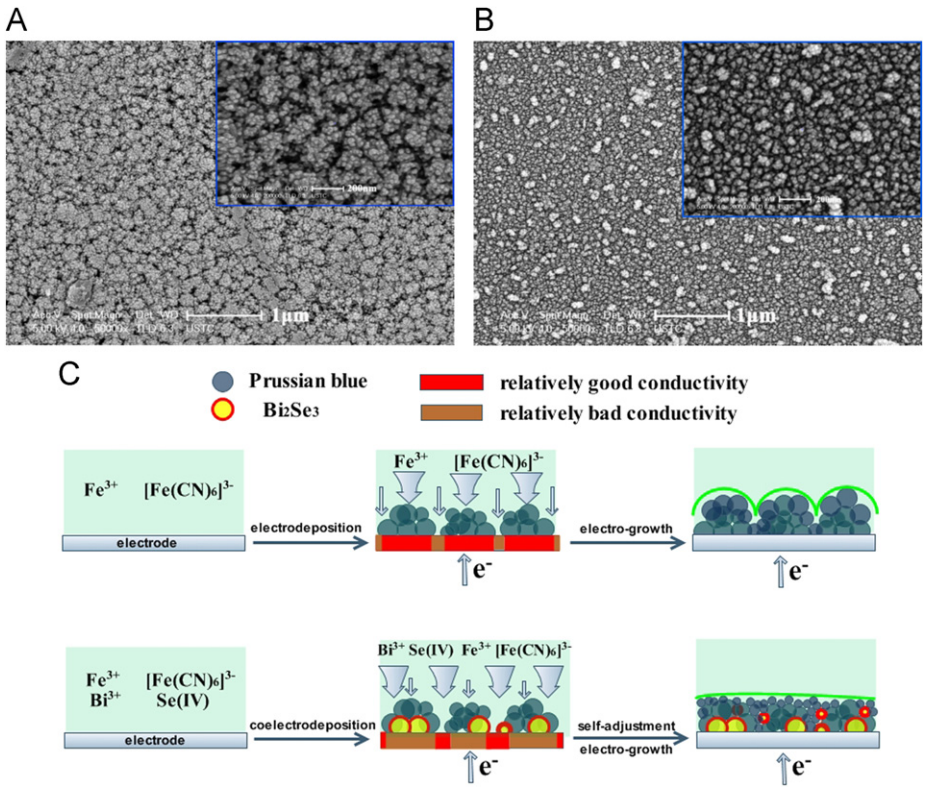

Fig. 3. SEM images of (A) Prussian blue and (B) PB/Bi_2Se_3 films electrodeposited on glass carbon slice. Inset shows the amplified images. (C) Schematic representation of the preparations of pure PB (above) and PB/Bi_2Se_3 hybrid film (below) for possible mechanism explanation.

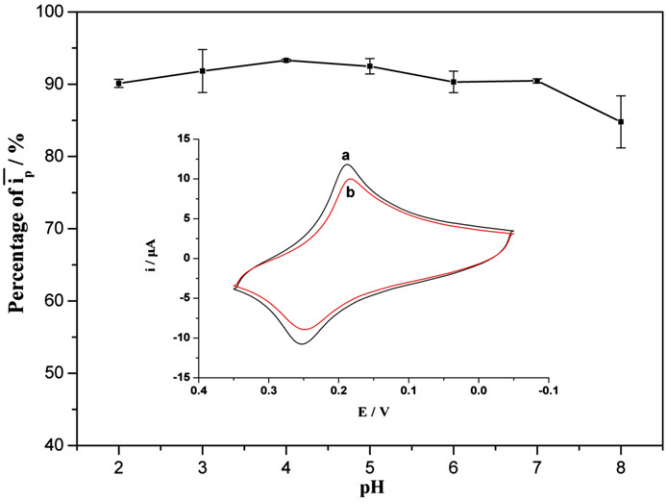

Fig. 4. Electrochemical stability of the PB/Bi_2Se_3 hybrid film at different pH solutions evaluated from CV peak currents. Conditions: supporting electrolyte, 0.025 M phosphate buffer with different pHs and 0.1 M KCl; potential scan rate, 100 mV s^{-1}; number of cycles, 200. Inset shows the CV curves at pH 8.0, a and b represent the first and the 200th cycle, respectively.

at alkaline pH, attributing to the homogeneous and spontaneous reaction (Ricci and Palleschi, 2005). Besides, Bi_2Se_3 particles have been synthesized by chemical method in alkaline solution, which means they are alkaliresistant (Sankapal et al., 2000). Thus, this excellent pH stability could be due to the compact hybrid film, whose structure may be similar to that obtained by chemical deposition of stable PB, and to the alkaline stable and surface-conductive Bi_2Se_3 nanoparticles in hybrid film, which act as cornerstones restricting any well-bound PB leaking and minimise the pH effect.

In order to investigate the amperometric stability of PB/Bi_2Se_3 hybrid film, the percentages of the decrease in amperometric responses in PBS (pH6.86) were recorded after 30 times addition of 50 μM H_2O_2. As shown in SFig. 5, four parallel detections gave the results that the response remained over 85% of its initial value after 30 assays of 50 μM H_2O_2, which means there was no serious leaching of Prussian blue from the PB/Bi_2Se_3 hybrid film.

3.4. *Electrochemical sensing of H_2O_2 at PB/Bi_2Se_3 hybrid film*

Sensitive measurement of H_2O_2 is of great importance both in biological study and in the development of electrochemical biosensors since, as one kind of reactive oxygen species, H_2O_2 plays a great role in the biological processes. The electrochemical sensing of H_2O_2 of PB/Bi_2Se_3 hybrid film was, first of all, studied with the addition of H_2O_2 into the electrochemical cell using the PB/Bi_2Se_3/GCE as working electrode in 0.025 M PBS and 0.1 M KCl of pH 6.86 which is close to physiological pH. Inset of Fig. 5(A) shows the CVs of PB/Bi_2Se_3/GCE in PBS with different H_2O_2 concentrations. It was shown that increasing the concentration of H_2O_2, the reduction currents at about 0.15 V dramatically increased and the oxidation peak currents gradually decreased compared with that on the control without H_2O_2, indicating the electrocatalytic activity of the thus-prepared PB/Bi_2Se_3 hybrid film towards the H_2O_2 reduction.

To investigate the contribution of Bi_2Se_3 in the hybrid film to the electrocatalytic of H_2O_2, the current changes of pure Bi_2Se_3/GCE to different concentrations of H_2O_2 were examined, as shown in SFig. 6. However, only slight change was observed after adding some H_2O_2 under the potential scanning from +0.6 V to −0.1 V, which indicated that Bi_2Se_3 cannot catalyze the reduction of H_2O_2. Therefore, it could be easily deduced that the good electrocatalytic property of PB/Bi_2Se_3 may mainly be attributed to the good sensitivity of PB nanoparticles. After activation by CV scanning in 0.1M KCl, the more stable PB particles were formed (Roig et al., 1994). According to

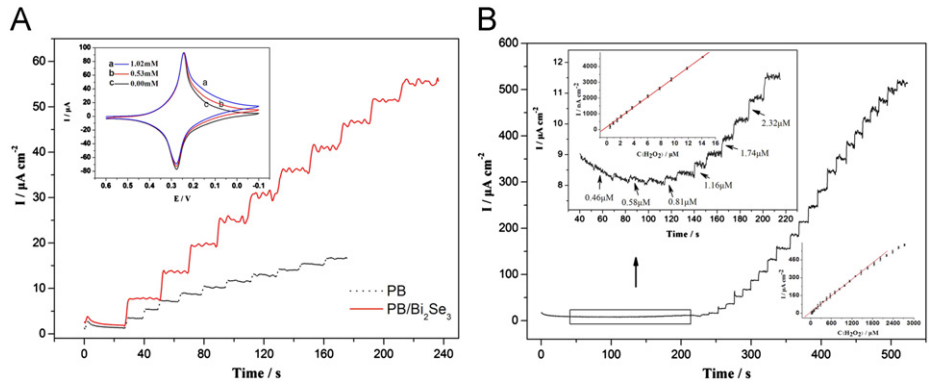

Fig. 5. (A) Amperometric response of PB/Bi_2Se_3 and PB films to 10 times addition of 30 μM H_2O_2 at the working potential of 0.00 V. Inset is the CVs of PB/Bi_2Se_3 at various concentration of H_2O_2 in 0.025 M PBS and 0.1 M KCl at a potential scan rate of 90 mV s^{-1}. (B) Amperometric response of PB/Bi_2Se_3 film to successive addition of 0.232 mM (low concentration) and 23.16 mM (high concentration) H_2O_2 into a 20 mL supporting electrolyte. Inset gives the amplification of ultrasensitive response to the low concentration of H_2O_2 and two linear curves. Applied potential: 0.00 V (see SFig. 7).

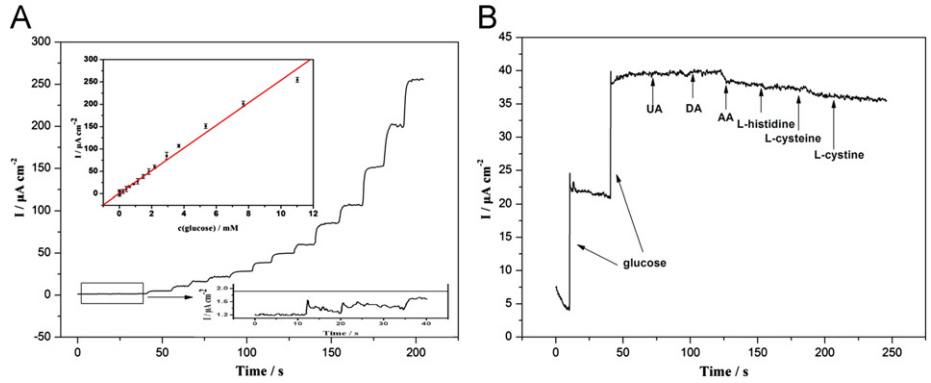

Fig. 6. (A)Typical amperometric response of the biosensor to different concentrations of glucose into a 15 mL stirring base solution (0.025 M PBS and 0.1 M KCl, pH 6.86). Inset above shows the calibration curve of the biosensor as a function of glucose concentration. Inset below is the enlarged view of the response to the low concentration of glucose. Applied potential: 0.00 V. (B) Chronoamperometric response to the injection of 0.70 mM glucose and six common interferences: 0.20 mM uric acid (UA), 0.20 mM dopamine (DA), 0.20 mM ascorbic acid (AA), 0.20 mM L-histidine, 0.20 mM L-cysteine and 0.20 mM L-cystine. The working potential was 0.00 V.

literature (Garjonyte and Malinauskas, 1998), the catalytic mechanism could be described as follows:

$$\underset{\text{Prussian blue}}{KFe^{(III)}[Fe^{(II)}(CN)_6]} + e^- + K^+ \leftrightarrow \underset{\text{Prussian white}}{K_2Fe^{(II)}[Fe^{(II)}(CN)_6]} \quad (1)$$

$$\underset{\text{Prussian white}}{2K_2Fe^{(II)}[Fe^{(II)}(CN)_6]} + H_2O_2 + 2H^+ \leftrightarrow \underset{\text{Prussian blue}}{2KFe^{(III)}[Fe^{(II)}(CN)_6]} + 2H_2O + 2K^+ \quad (2)$$

Chronoamperometry was employed to investigate quantitatively the response characteristics of the sensor to H_2O_2. Amperometric response of the PB/Bi_2Se_3 modified electrode to 10 times successive addition of 100 μM H_2O_2 was shown in Fig. 5(A) under optimized experimental conditions, with the PB modified electrode as the control at the same condition. Obviously, the response of H_2O_2 at PB/Bi_2Se_3 hybrid film is about 3 times as much as that at PB film, which is probably due to the nano-size effect of Prussian blue nanoparticles. With the successive addition of H_2O_2 to a gently stirred 0.025 M PBS containing 0.1 M KCl (pH 6.86), the reduction current increased steeply and then achieved 95% of the steady-current in less than 1 s which indicates that the response was very fast. Two good linear relationships of the sensor to H_2O_2 were obtained from 0.46 to 14.12 μM with R^2 of 0.9977 for low concentration range (sensitivity of 318.5 μA mM^{-1} cm^{-2}) and 23.27 to 2024 μM with R^2 of 0.9991 for high concentration range (sensitivity of 247.2 μA mM^{-1} cm^{-2}). The detection limit was estimated to be 81.3 nM on the basis of the signal-to-noise characteristics (S/N=3). These results show that PB/Bi_2Se_3 based electrochemical platform exhibits the fast and sensitive detection of H_2O_2 in a good linear range, indicating that PB/Bi_2Se_3 is an excellent material for the enhanced electrochemical determination of H_2O_2.

3.5. Electrochemical detection of glucose on the GOD-CS/PB/Bi_2Se_3 biosensor

Chitosan (CS) is a non-acetylated or partially deacetylated chitin. It can be found in the fungal cell wall and the exoskeletons of lots of arthropods such as crabs and shrimps. Due to its excellent film-forming ability, biocompatibility, well mechanical strength, cheapness and a susceptibility to chemical modifications, it has been widely used for immobilization of enzymes and to fabricate amperometric biosensors (Chen and Gorski, 2001; Chen et al., 2003; Miao and Tan, 2001; Wang et al., 2009). Based on the excellent electrocatalytical activity of PB/Bi_2Se_3 hybrid film to H_2O_2, in further work, the chitosan membrane containing GOD was immobilized on the PB/Bi_2Se_3 modified electrode by drop-coating method to construct the GOD-CS/PB/Bi_2Se_3 biosensor. Considering that chitosan would become insoluble which could be beneficial to the stability of the biosensor when pH is higher than pK_a of 6.3 (Sorlier et al., 2001), the buffer solution of pH 6.86 was chosen for the detection of glucose in this experiment. Fig. 6(A) shows the amperometric response of the biosensor to glucose in air-saturated stirring PBS (pH 6.86) and the corresponding calibration curve of the biosensor as a function of glucose concentration. The time required for reaching 95% steady-state

response was within 3 s. The inset in Fig. 6(A) shows a good linear response in the range of 0.01–11.02 mM glucose with a correlation coefficient of 0.9940 and the sensitivity of 24.55 $\mu A\,mM^{-1}\,cm^{-2}$. The regression equation is $I\ (\mu A\,cm^{-2}) = 2.01 + 24.55C_{glucose}\ (mM)$. The detection limit can be estimated for 3.8 μM defined from a signal/noise of 3. Its relative standard deviation (RSD) is 2.37% for seven successive determinations in 0.5 mM glucose solution. It is worth to mention that a wider linear range for glucose at GOD-CS/PB/Bi_2Se_3 film does not agree well with that for H_2O_2 at PB/Bi_2Se_3 film. The reason may be that the response current at the biosensor comes from the enzymatically liberated H_2O_2. In other words, the glucose added is partly converted to H_2O_2 via the enzymatic reaction.

Together with the fabrication time, the analytical performance of this proposed biosensor was compared with other glucose biosensors listed in Table S1. It could be easily seen that the proposed biosensor exhibits high sensitivity, wide linear range and low limit of detection.

As shown in Fig. 6(B), there is no significant change of the response current to be observed by adding six common interferences into glucose solution, indicating that thus-fabricated biosensor has good anti-interferential ability. The stability of the resulting biosensor was evaluated by reduplicative measurement, and the biosensor was stored dryly at 4 °C when not used. Only slight decrease for the current which will retain 90% of its initial value was found after two months, indicating that the long-term stability of the resulting biosensor was satisfactory.

In order to illustrate the practical utility of this glucose biosensor, human serum samples were assayed. Fresh serum samples were provided by a local hospital, which were firstly analyzed with a standard clinical assay which is based on glucose dehydrogenase electrode method. Then serum samples of 200 μL were successively added into 10 mL phosphate buffered saline, and the response were obtained at 0.00 V. As shown in Table S2, good agreement between the two sets of data allows us to ascertain the practical utility of the fast-fabricated biosensor. It is feasible to apply this biosensor to determine glucose in real samples. Besides, within the error limit, there appears to be no statistically significant difference between these two methods (assuming significance level of 0.05), which means the traditional glucose dehydrogenase electrode could be replaced by this novel biosensor.

4. Conclusions

A Prussian blue/topological insulator Bi_2Se_3 hybrid film has been prepared by coelectrodeposition technique. It was found that topological insulator Bi_2Se_3 has the advantages in assisted synthesis of smaller nanoparticles and smoother film surface. PB nanoparticles in this hybrid film were very stable during the raise of pH, even in the alkalescent solution of pH 8.0. This novel hybrid film also showed a big value of electron transfer rate constant and exhibited good sensibility as well as low detection limit to detection of H_2O_2. An amperometric glucose biosensor has been logically fabricated by dropping GOD-CS solution on the hybrid film. From its excellent performance to the detection of glucose and the practical utility to the real serum samples, it can be concluded that this simple but powerful hybrid film possesses of the potential application in biosensor design for accurate and tight monitoring to diabetes mellitus.

Acknowledgments

This work was financially supported by the National Natural Science Foundation of China (no. 20975095).

Appendix A. Supplementary material

Supplementary data associated with this article can be found in the online version at http://dx.doi.org/10.1016/j.bios.2012.06.001.

References

Bernevig, B.A., Hughes, T.L., Zhang, S.C., 2006. Science 314, 1757–1761.
Cha, J.J., Williams, J.R., Kong, D.S., Meister, S., Peng, H., Bestwick, A.J., Gallagher, P., Goldhaber-Gordon, D., Cui, Y., 2010. Nano Letters 10, 1076–1081.
Chen, L., Gorski, W., 2001. Analytical Chemisry 73, 2862–2868.
Chen, X., Jia, J.B., Dong, S.J., 2003. Electroanalytical Chemistry 15, 608–612.
Cui, H.M., Liu, H., Wang, J.Y., Li, X., Han, F., Boughton, R.I., 2004. Journal of Crystal Growth 271, 456–461.
Cui, X.P., Hong, Li., Lin, X.Q., 2002. Journal of Electroanalytical Chemistry 526, 115–124.
Domínguez-Vera, J.M., Colacio, E., 2003. Inorganic Chemistry 42, 6983–6985.
Fu, L., Kane, C.L., 2007. Physical Review B 76, 045302.
Garjonyte, R., Malinauskas, A., 1998. Sensors and Actuators B: Chemical 46, 236–241.
Harman, T.C., Paris, B., Miller, S.E., Goering, H.L., 1957. Journal of Physics and Chemisty of Solids 2, 181–190.
Haghighi, B., Hamidi, H., Gorton, L., 2010. Sensors and Actuators B: Chemical 147, 270–276.
König, M., Wiedmann, S., Brüne, C., Roth, A., Buhmann, H., Molenkamp, L.W., Qi, X.L., Zhang, S.C., 2007. Science 318, 766–770.
Karyakin, A.A., 2001. Electroanalytical Chemistry 13, 813–819.
Karyakin, A.A., Gitelmacher, O.V., Karyakina, E.E., 1995. Analytical Chemistry 67, 2419–2423.
Karyakin, A.A., Karyakina, E.E., Gorton, L., 2000. Analytical Chemistry 72, 1720–1723.
Karyakin, A.A., Puganova, E.A., Budashov, I.A., Kurochkin, I.N., Karyakina, E.E., Levchenko, V.A., Matveyenko, V.N., Varfolomeyev, S.D., 2004. Analytical Chemistry 76, 474–478.
Kong, D.S., Randel, J.C., Peng, H.L., Cha, J.J., Meister, S., Lai, K.J., Chen, Y.L., Shen, Z.X., Manoharan, H.C., Cui, Y., 2009. Nano Letters 10, 329–333.
Laviron, E., 1979. Journal of Electroanalytical Chemistry and Interfacial Electrochemistry 101, 19–28.
Lin, Y.F., Chang, H.W., Lu, S.Y., Liu, C.W., 2007. Journal of Physical Chemistry C 111, 18538–18544.
Miao, Y., Tan, S.N., 2001. Analytica Chemica Acta 437, 87–93.
Moore, J., 2009. Nature Physics 5, 378–380.
Moore, J.E., 2010. Nature 464, 194–198.
Peng, H.J., Zhou, J.L., Tang, D., Lai, Y.Q., Liu, F.Y., Li, J., Liu, Y.X., 2011. Electrochimica Acta 56, 5085–5089.
Reach, G., Wilson, G.S., 1992. Analytical Chemistry 64, 381A–386A.
Ricci, F., Palleschi, G., 2005. Biosensors and Bioelectronics 21, 389–407.
Roig, A., Navarro, J., Garcia, J.J., Vicente, F., 1994. Electrochimica Acta 39, 437–442.
Sankapal, B.R., Mane, R.S., Lokhande, C.D., 2000. Materials Chemistry and Physics 63, 230–234.
Satterthwaite, C.B., Ure Jr., R.W., 1957. Physical Review 108, 1164–1170.
Sorlier, P., Denuzière, A., Viton, C., Domard, A., 2001. Biomacromolecules 2, 765–772.
Subramanian, S., Padiyan, D.P., 2008. Materials Chemistry and Physics 107, 392–398.
Torane, A.P., Bhosale, C.H., 2001. Materials Research Bulletin 36, 1915–1924.
Wang, D.B., Yu, D.B., Mo, M.S., Liu, X.M., Qian, Y.T., 2003. Journal of Crystal Growth 253, 445–451.
Wang, J., 2002. Sensors Update 10, 107–119.
Wang, J., 2007. Chemical Reviews 108, 814–825.
Wang, X.Y., Gu, H.F., Yin, F., Tu, Y.F., 2009. Biosensors and Bioelectronics 24, 1527–1530.
Wu, S.G., Liu, J.P., Bai, X., Tan, W.G., 2010. Electroanalytical Chemistry 22, 1906–1910.
Xia, Y., Qian, D., Hsieh, D., Wray, L., Pal, A., Lin, H., Bansil, A., Grauer, D., Hor, Y.S., Cava, R.J., Hasan, M.Z., 2009. Nature Physics 5, 398–402.
Xiao, F., Hangarter, C., Yoo, B., Rheem, Y., Lee, K.H., Myung, N.V., 2008. Electrochimica Acta 53, 8103–8117.
Zhang, H.J., Liu, C.X., Qi, X.L., Dai, X., Fang, Z., Zhang, S.C., 2009. Nature Physics 5, 438–442.